American Mineralogist, Volume 62, pages 565–573, 1977

The decarbonation of carbonate–fluorapatite (francolite)

ALAN MATTHEWS

Department of Geology
The Hebrew University of Jerusalem, Israel

AND YAACOV NATHAN

Geochemistry Division, Geological Survey of Israel
Jerusalem, Israel

Abstract

The decarbonation of carbonate–fluorapatite (francolite) has been studied in the range 599°–747°C, at atmospheric pressure. Progressive CO_2 loss from the apatite is characterized by color change, an increase in crystallinity, and the appearance of an anomalous ν_2 doublet in the infrared absorption spectrum. Interpretation of the rate data with diffusion theory gives an activation energy of 62.5 kcal/mole and entropy of activation within the limits 3.8 to 11.2 cal/mole/deg. Significant deviations from ideal kinetics occur at high fractional CO_2 losses. Application of the data to the thermometry of the 'Mottled Zone' (Israel) thermal metamorphism gives 300°C as a minimum temperature estimate for the event. Optimum conditions are suggested for industrial processes which concentrate phosphorites by roasting.

Introduction

Carbonate–fluorapatite (francolite) is the principal mineral of phosphorites, the sedimentary rock phosphates. The nature of the carbonate content, whether it is part of the apatite, or adsorbed on the surface of the mineral, or even due to admixture with $CaCO_3$, and its structural position, if it is part of the apatite lattice, has been a subject of considerable controversy, which today appears to be resolved. The CO_3^{2-} group is considered to be a part of the fluorapatite structure, substituting for PO_4^{3-} groups in the naturally occurring mineral (McConnell, 1952a; Altschuler *et al.*, 1952; LeGeros *et al.*, 1970). The structure of carbonate–fluorapatite is probably triclinic (pseudohexagonal), and upon heating it decomposes according to the following reaction (Axelrod, private communication):

$$Ca_{5-1/2x}[(PO_4)_{3-x}(CO_3)_x](F, OH) \rightarrow$$
(carbonate–fluorapatite)
$$Ca_5(PO_4)_3(F,OH) + CaO + CO_2$$
(fluorapatite)

The presence of CaO as a separate phase in the product has been confirmed in the present study; the X-ray powder pattern of CaO can be recognized in the heated sample. It should be emphasized that the formula given above for carbonate–fluorapatite is schematic, since at least some Na substitutes for Ca, F usually occurs above the stoichiometric value, and hydroxyl also occurs in minor amounts. Also the CaO does not form in the same proportion as the liberated CO_2; less CaO is formed, and the CaO/P_2O_5 ratio in the heated material is greater than stoichiometric.

The rate of decarbonation of carbonate–fluorapatite has been experimentally studied in the temperature range 599°–747°C, at atmospheric pressure. The objectives of the study were to investigate the mineralogy and kinetics of the solid-state reaction. The data can then be used to provide a geological thermometer when sedimentary rocks containing carbonate–fluorapatite are metamorphosed. The study may also be of use in setting optimal conditions for industrial processes which use heat to enrich phosphorites.

Experimental methods

The raw material is the product called by the Negev Phosphate Company 'Cyclone Makhtesh.' It is the small-size fraction of the Makhtesh Katan phosphorite which is separated by St. Jacques cy-

clones. It contains approximately 30 percent P_2O_5, and the following impurities: calcite, organic matter, montmorillonite, quartz, some gypsum, and traces of halite. The raw material was repeatedly washed with distilled water, and the clay fraction (less than 2 μm) was decanted. This treatment removed montmorillonite, quartz (which occurs in the clay fraction), gypsum, and halite. The remaining material was treated with triammonium citrate (Silverman *et al.*, 1952) to dissolve the calcite. Table 1 gives partial chemical analyses of the sample before and after this treatment. The washed and dried residue was carefully homogenized and preheated at 440°C for 5 hours. Infrared absorption spectra, which can detect as little as 0.1 percent $CaCO_3$, did not show any extraneous peaks apart from organic matter. The organic matter appeared to be intimately mixed with the phosphate, and it was not possible to separate it by mechanical means. A grain-size analysis was carried on the treated material using a Warman cyclosizer (Table 2). This sample was used in all experiments.

For each experimental run, 500 mg of the pretreated reactant was weighed into a small vitreous silica crucible. The crucible and its contents were then inserted into a carefully calibrated horizontal furnace whose temperature was precisely maintained by means of a thyristor fired P.I.D. controller (West Gardian). Temperature was monitored automatically every few minutes by a Honeywell versaprint recorder connected to a chromel–alumel thermocouple, whose tip was in contact with the crucible. Accurate temperature measurements were made with a Leeds and Northrup K-4 potentiometer. Samples reached temperature within 2 minutes after being inserted into the furnace. On completion of the experiments, the products were cooled in air and immediately reweighed to determine the weight loss.

The product was examined by X-rays and the angular difference between the two X-ray diffraction peaks (410) and (004) measured. This $\Delta 2\theta$ has been shown by Gulbrandsen (1970) to be a linear function of the CO_2 content of the apatite. The $\Delta 2\theta$(004)–(410)

Table 1. Partial chemical analyses of the reactant before and after treatment with triammonium citrate

	Wt. % P_2O_5	Wt. % F	Wt. % CO_2	Wt. % H_2O
Before treatment	33.4	3.8	5.5	1.1
After treatment	35.4	4.0	3.9	1.1

Table 2. Grain-size distribution of the purified reactant

	Size Fraction				
	2–10μm	10–20μm	20–30μm	30–40μm	40–60μm
Percentage	53	13	9	10	15

measurements were made on chart recordings of runs of 0.5°C per minute traverses, using an XRD-6 General Electric diffractometer with Ni-filtered Cu radiation (Fig. 3). Infrared absorption spectra for many samples were made on a Perkin-Elmer IR 257. The samples were mixed with KBr (in concentration of about 2 mg sample/200 mg KBr) and made into pellets. The range covered was from 625–4000 cm^{-1}. A simultaneous DTA/TGA analysis was made on a Mettler Thermoanalyser, and some selected heated samples were examined with a Cambridge Stereoscan (S.E.M.).

Results and discussion

The original material is yellow-cream in color. The pretreatment at 440°C changes the color to grey, due to reduction of the organic matter. Above 550°C, the reduced organic matter is quickly oxidized and color changes to white. Above this temperature, CO_2 also begins to leave the structure in measurable amounts. Heating at high temperatures gives the apatite a greenish tint. This coloration may be due to the production of electronic defects (vacancies?) and not to the presence of trace elements, since the coloration is common to all heated phosphorites, irrespective of their origin, and prolonged exposure to X-rays also gives a greenish tint to some apatites.

Table 3 summarizes the weight loss and $\Delta 2\theta$(004)–(410) data for the four experimental temperatures. The fractional weight loss (α) is also included in the table. The total experimental weight loss exceeds the actual CO_2 content (Table 1) by 1.3 percent. Independent analysis showed this difference to be due mainly to the partly reduced organic matter, and in part to water loss. Organic matter analysis by a modified Pregl method gave carbon = 1.0 percent and hydrogen = 0.1 percent; the total water content of the apatite = 1.1 percent (Table 1). Of this water, 0.2 percent is hydroxyl substituting for F, and is not expelled even at the highest experimental temperature. Pretreatment removes 0.5 percent. Part of the remaining water (0.4%) is due to the oxidation of organic H during the Penfield analysis, and the remainder contributes to the weight loss. The weight

loss arising from decarbonation is calculated by subtracting the organic matter and water weight loss from the total. To avoid significant overlapping between the CO_2 and other weight losses, no total weight loss below 2 percent was considered. The errors in the decarbonation weight losses given in Table 3 cannot exceed 0.1 percent.

Figure 1 shows the CO_2 weight loss as a function of time for the various temperatures. The initial rapid decarbonation is followed by a much slower late-stage CO_2 loss. The TGA/DTA analysis indicated a single continuous endothermic process. Figure 2 shows $\Delta 2\theta$(004)–(410) as a function of the CO_2 content deduced from weight loss. The agreement with Gulbrandsen's line is remarkably good. It can be noted that at very low CO_2 values (less than 0.2%) the relation breaks down; this may be expected, since small amounts of carbonate can be accommodated in the apatite structure without any distortion. Another observation from the X-ray diffractograms is the increase of crystallinity which occurs as the CO_2 is expelled. Textural examination with the S.E.M. shows that continuous heating results in the development of crystalline faces on the surface of the apatite grains.

The infrared absorption spectra furnish complementary evidence to the X-ray diffractograms, because they are very sensitive to changes in small amounts of CO_2 ($\leq$ 1%), but are relatively insensitive to higher CO_2 contents (Fig. 4). Heated samples with low CO_2 contents give an anomalous ν_2 doublet at 867 and 877 cm^{-1} (Fig. 4B). This doublet is well known in the spectra of biological apatites, but is anomalous since the CO_3^{2-} ν_2 vibration is normally nondegenerate. LeGeros *et al.* (1970) discuss at length the various explanations for this phenomena. The fact that the doublet is not observed at first with high CO_2 content (Fig. 4A), and appears only at low CO_2 content, supports in our opinion McConnell's (1952b) hypothesis that CO_3^{2-} groups in the apatite are in two different orientations "perpendicular" and "parallel" to the c axis (both groups are in fact tilted at ~32°C). In accordance with the observed negative birefringence, most CO_3^{2-} are perpendicular and only a few are parallel. Structurally, it is easier to expel the perpendicular groups, and the effect of the parallel carbonate groups is only seen when a greater part of the perpendicular CO_3^{2-} are lost.

Kinetics of decarbonation

The kinetics of the decarbonation reaction can be interpreted from the experimental data. In the analy-

Table 3. Results of decarbonation experiments at 1 atmosphere

Run No.	Time (Hrs.)	Wt. Loss* %	$\Delta 2\theta$ (004)-(410)	Fractional+ CO_2 Loss
T=599±4°C				
30	12.33	0.94	1.41	0.24
25	16.00	1.17	1.42	0.30
33	24.00	-	1.44	-
31	24.33	1.64	1.44	0.42
29	31.50	1.70	1.46	0.44
26	40.00	1.92	1.48	0.49
21	48.00	-	1.48	-
35	48.33	2.09	1.49	0.54
23	56.33	2.09	1.51	0.54
22	64.50	1.98	1.51	0.51
36	72.00	2.38	1.50	0.61
20	72.00	2.31	1.52	0.59
28	88.00	2.41	1.54	0.62
34	97.00	-	1.54	-
24	104.00	2.69	1.56	0.69
T=649±4°C				
69	0.50	-	1.36	-
52	2.00	1.48	1.43	0.38
53	4.25	2.39	1.45	0.61
55	8.00	2.63	1.49	0.67
56	12.50	2.87	1.52	0.74
49	18.00	2.95	1.53	0.76
68	45.00	3.12	1.53	0.80
50	48.00	2.97	1.56	0.76
51	92.00	3.38	1.57	0.87
T=698±4°C				
66	0.27	1.35	1.42	0.35
46	0.50	2.04	1.45	0.52
44	1.05	2.59	1.50	0.66
42	2.00	2.88	1.55	0.74
47	4.00	3.21	1.54	0.82
40	6.00	3.19	1.58	0.82
41	16.00	3.37	1.58	0.86
67	23.00	3.53	-	0.90
45	24.20	3.25	1.59	0.83
43	48.20	3.56	1.57	0.91
48	92.00	3.74	1.60	0.96
T=747±4°C				
64	0.17	2.40	1.53	0.62
58	0.25	2.79	1.54	0.72
57	0.50	3.21	1.57	0.82
61	1.00	3.31	1.58	0.85
62	4.00	3.40	1.58	0.87
65	8.00	3.55	1.59	0.91
59	20.00	3.76	1.58	0.96
60	44.00	3.86	1.60	0.99
63	72.00	3.89	1.59	1.00

* Calculated by subtracting the organic matter and water content from the total weight loss.

\+ Calculated by dividing the CO_2 weight loss by the CO_2 content of the reactant (cf. Table 1).

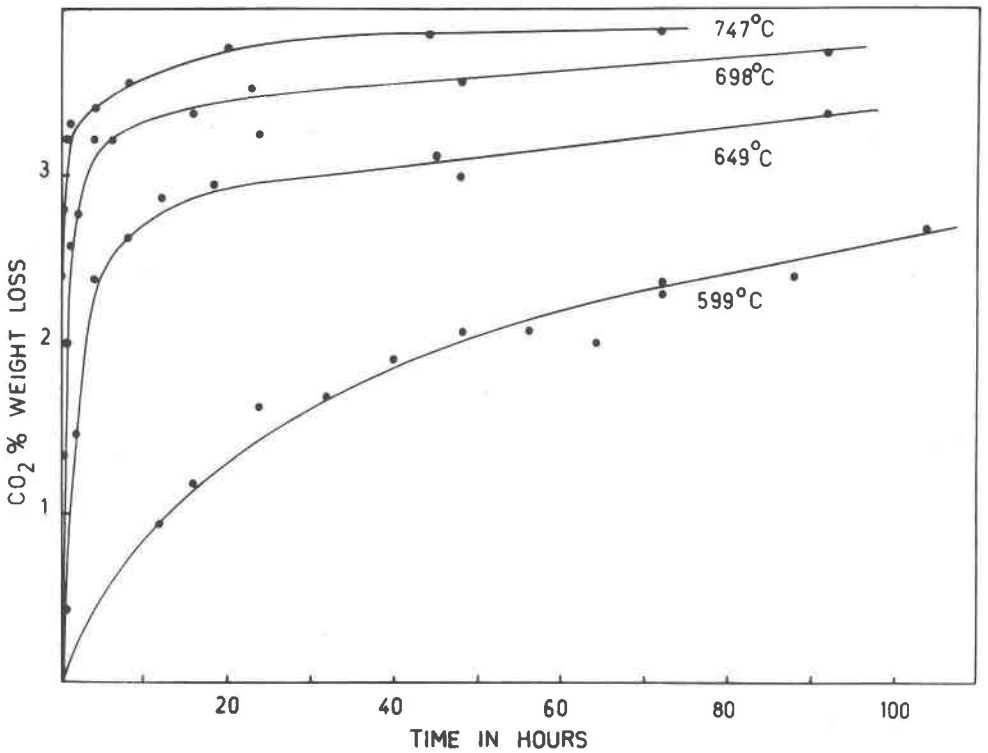

Fig. 1. Plots of CO_2 percent weight loss against time for the experimental data at each temperature.

sis that follows, the weight loss results are used in preference to the $\Delta 2\theta(004)$–(410) because of the greater sensitivity of the weight measurements to small CO_2 losses, especially for high fractional CO_2 losses to which the X-ray measurements are particularly insensitive.

The initial question posed is: are the kinetics of decarbonation controlled by diffusion of CO_2 out of the apatite, or by an alternative process such as disproportionation of CO_2 from the lattice? Martin and Fyfe (1970) have provided a simple graphical method for analyzing heterogeneous reaction kinetics, which can be applied to the experimental data of this study. For an "Interface" controlled reaction (after Bratton and Brindley, 1965)

$$(1) \quad I_\alpha = K_I t = [1 - (1 - \alpha)^{1/3}] = 0.206\ (t/t_{0.5})$$

α is the fractional extent of conversion to product (fractional weight loss) and $t_{0.5}$ is the time for 50 percent reaction. Equation (1) describes the development, at a constant rate, of an interface which penetrates inwards into a spherical particle. In applying this model to the decarbonation kinetics it is assumed that the reaction interface represents a boundary or zone separating decarbonated material from reactant. The second model (after Jander, 1927) is based on parabolic kinetics and describes a reaction progress controlled by diffusional processes.

$$(2) \quad D_\alpha = K_D t = [1 - (1 - \alpha)^{1/3}]^2 = 0.0426\ (t/t_{0.5})$$

Both models neglect nucleation effects. The half-time ($t_{0.5}$) is evaluated from experimental α *vs.* time plots. The D_α and I_α functions can be represented on plots of α *vs.* $(t/t_{0.5})$, and comparison of the experimental data with the two model curves leads to an interpretation of the critical rate processes. Analysis of the experimental decarbonation data (Table 3) shows that at all temperatures the D_α model is followed more closely (Fig. 5). At 599°C all data plot close to the D_α curve (Fig. 5A), but at the higher temperatures the data deviate away from the D_α line for high α values (Fig. 5B). The significance of these deviations will shortly be considered. However, it is evident from the above analysis that the rate-controlling process is the diffusion of CO_2 out of the fluorapatite.

Diffusional kinetics are described by the Arrhenius exponential function:

$$(3) \quad D = D_o \exp(-E_A/RT)$$

D is the diffusion coefficient (cm^2/sec), D_o is a tem-

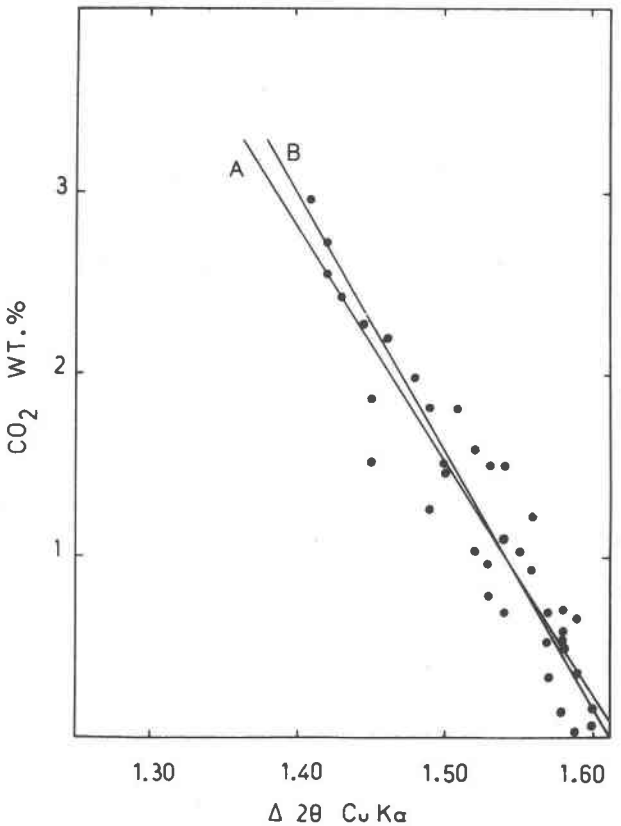

Fig. 2. Plot of $\Delta 2\theta$(004)–(410) against CO_2 weight percent (obtained by subtracting the CO_2 weight loss from the CO_2 content of the reactant), for all experimental data. *A* is the linear regression line deduced from the plot:

$y = 20.85 - 12.88x$ (y = CO_2 wt.%, $x = \Delta 2\theta$, esd = 0.263).

B is the line deduced by Gulbrandsen (1970) from X-ray and chemical analyses of marine apatites.

perature-independent pre-exponential factor, R is the gas coefficient, T is the absolute temperature, and E_A is the activation energy. Evaluation of a pre-exponential factor and E_A is necessary for the extrapolation of experimental kinetic data onto the geological time scale. It is possible to estimate approximately these coefficients from equations (2) and (3). However, an intrinsically more useful analysis can be made using an equation based on the conduction of heat in solids. Diffusion of CO_2 from a spherical particle can be described by the equation (*cf.* Carslaw and Jaeger, 1959, p. 233–237):

$$(4) \quad 1 - \alpha = (6/\pi^2) \sum_{n=1}^{n=\infty} [(1/n^2) \times \exp(-n^2 \pi^2 Dt/a^2)]$$

in which a is the radius of a spherical particle. The model represented by (4) corresponds more closely to the mechanism of decarbonation than does the Jander model (2). Solution of equation (4) is best approached by drawing master plots of α *vs.* (Dt/a^2); these can be done by substituting known values of (Dt/a^2) into (4) and summing for α. (Dt/a^2) can be evaluated for the experimental α from these master plots. These (Dt/a^2) values are then plotted against the experimental time, yielding a straight line with slope (D/a^2) passing through the axes. Finally, a plot of $\log_{10}(D/a^2)$ *vs.* $(1/T)$ gives a straight line with slope $(-E_A/2.303R)$ and an intercept of $\log_{10}(D_o/a^2)$.

The CO_2 weight-loss data presented in Table 3 have been analyzed by the above procedure. The plots of (Dt/a^2) *vs.* time give good straight lines passing through the axes for all data at 599°C and for α values ≤ 0.75 at higher temperatures. Deviations from the ideal model at high α are very similar to those evident in Figure 5B. The (D/a^2) thus deduced

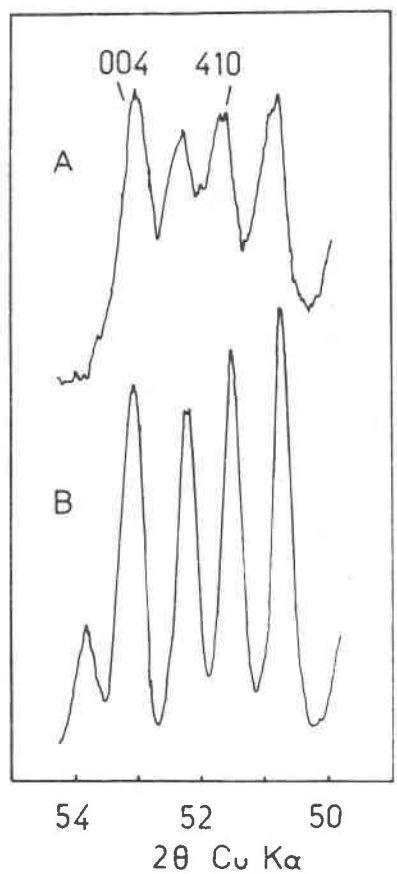

Fig. 3. X-ray diffractograms showing (004) and (410) reflections. (A) diffractogram of a sample with no CO_2 loss (#69); $\Delta 2\theta$ = 1.36. (B) diffractogram of a sample almost completely decarbonated (#63); $\Delta 2\theta$ = 1.59. Note the differences in crystallinity evident from the peak shapes.

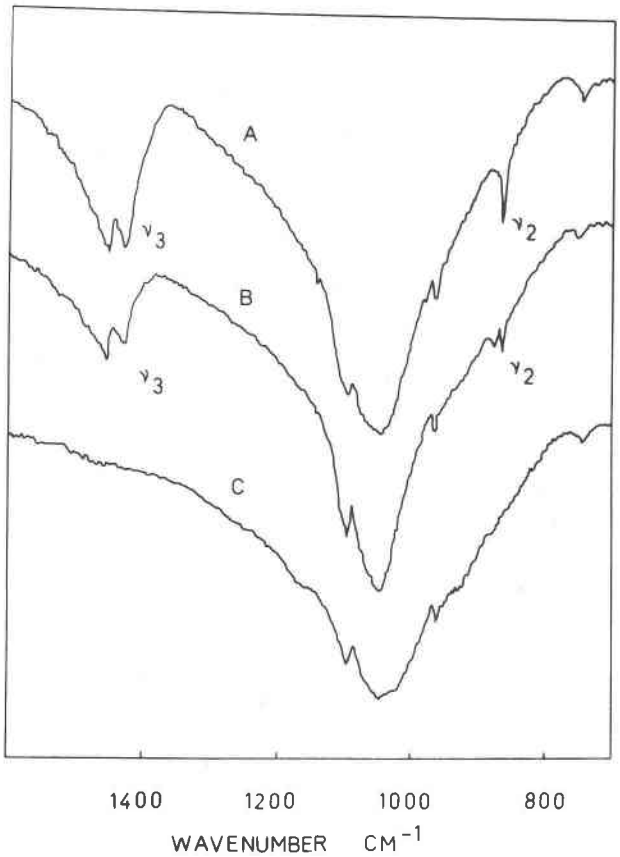

Fig. 4. Infrared absorption spectra of heated samples; (A) spectrum of sample containing 2.5% CO_2 (#66); (B) spectrum of sample containing 0.7% CO_2 (#57); (C) spectrum of completely decarbonated sample (obtained by calcining at 1000°C). Note the attenuation and final disappearance of the ν_3 peak with decreasing CO_2 content, and the appearance of a ν_2 doublet in spectrum B.

are analyzed in Figure 6 by a plot of $\log_{10}(D/a^2)$ *vs.* $(1/T)$. Linear regression gives a line whose slope yields an activation energy of 62.5 kcal/mole, and whose intercept a value of $(D_o/a^2) = 8.5 \times 10^8$.

Estimates of the entropy of activation (ΔS^*) can be made from a knowledge of the pre-exponential factor D_o. Absolute rate theory gives the following relationship (Wynne-Jones and Eyring, 1935):

$$(5) \qquad D_o = (kTd^2/2.72h) \times \exp(\pm\Delta S^*/R)$$

in which k is the Boltzmann constant, h is Planck's constant and d is the 'mean free path,' *i.e.* the distance between two successive equilibrium positions in the diffusion path. D_o for the decarbonation reaction is obtainable by dividing the experimental (D_o/a^2) by a^2. Analysis of the grain-size data (Table 2) indicates 5 μm to be a reasonable value for a. If the required d is taken to be a lattice parameter, the a-cell dimension (~10 A) is suitable, and the corresponding value of ΔS^* at 1000°K (727°C) is 11.2 cal/deg/mole. The choice of d implies that CO_2 diffuses out of the apatite by 'jumping' from one lattice position to another. However, the CO_2 more probably diffuses through defects, dislocations, interstices, and grain boundaries, rather than through the lattice. X-ray diffraction shows that the initial crystallite size is ~200 A, and subsequent heating results in an increase to ≥500 A, with corresponding annealing of the solid. The defect/dislocation density can thus be expected to be greatest in the initial stages of reaction, and 200 A can be taken as a maximum estimate of the mean free path. The corresponding value of ΔS^* at 1000°K is 3.8 cal/deg. The two calculated values place approximate limits on the actual entropy of activation. Whichever limiting value is taken, the decarbonation reaction is characterized by a favorable ΔS^*. This accords with the physical process of decarbonation for which an overall positive entropy change occurs owing to the release of CO_2.

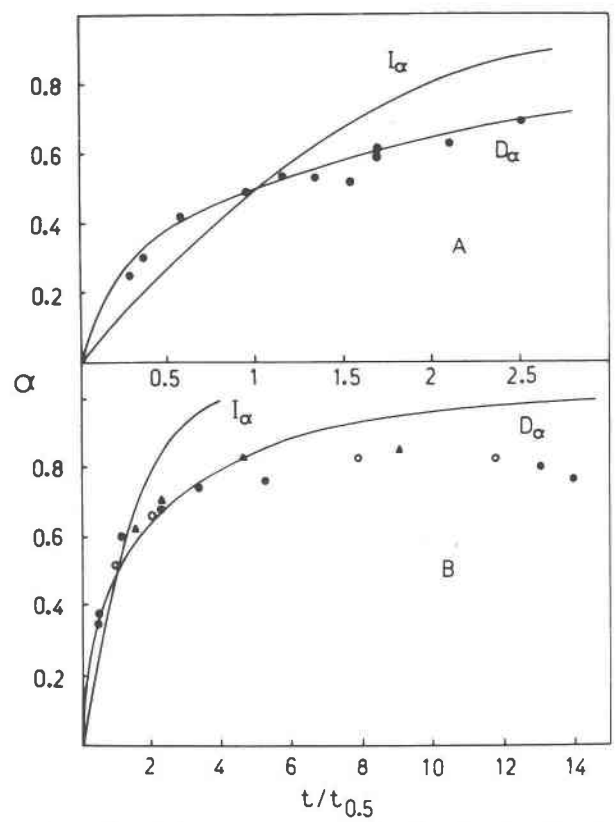

Fig. 5 Plot of the experimental fractional weight loss data (α) against ($t/t_{0.5}$). Derivation of the D_α and I_α model curves is given in the text. (A) data at 599°C; (B) data at higher temperatures (closed circles = 649°C, open circles = 698°C, triangles = 747°C).

The deviations at high α values from the 'ideal' diffusion kinetics originate from several possible sources. The first, breakdown in the model assumptions, has been discussed by Carter (1961). Failure of equation (4) can be expected to occur at high α, owing to its not allowing for differences in the molar volumes between reactant and product. However, Carter's analysis indicated that quite large molar volume differences were necessary for equation (4) to break down. Such large differences will not occur in the decarbonation reaction, and it is questionable if this effect applies. A second source for the deviations is the elimination of the small-size fraction from the reaction, since small particles will completely decarbonate before larger ones. This effectively increases the mean grain size, and examination of the exponential term in (4) shows that such an increase would result in low estimates of α. The overall grain size distribution is dominated by the 2–10 μm fraction (Table 2), and so this elimination effect will not be evident until substantial decarbonation has occurred.

A third and potentially significant source for the deviations is variation in the pre-exponential factor D_o. Any quantity which increases D_o during the course of reaction will result in the kinetics being retarded. A decrease in the entropy of activation would produce this effect, as would a reduction in the mean free path d. Crystallite size increases during reaction, with corresponding annealing and reduction in the defect/dislocation density. This would effectively reduce the mean free path of diffusion, and could also reduce ΔS^*, since this entropy term is related to the 'space' available for the activation process.

Finally, it can be noted that the deviations may also be related to the greater difficulty in expelling the "parallel" CO_3^{2-} groups relative to the more numerous "perpendicular" groups.

Applications and conclusions

The decarbonation data can be applied to the thermometry of the metamorphism of sediments containing carbonate–fluorapatite. One such application is to the metamorphism, known as the 'Mottled Zone (Israel) Event,' in which bituminous and phosphatic marls, chalks, limestones, sandstones, and conglomerates of Campanian to Neogene age were converted into a high-temperature mineral assemblage, notable for its exotic mineralogy (Bentor *et al.*, 1963a, b; Gross *et al.*, 1967; Gross, 1970; Kolodny *et al.*, 1973). The lack of an apparent cause for the metamorphism has led to some controversy over the origin of the 'Mottled Zone' assemblage, and indeed some authors have doubted the high-temperature genesis (*cf.* Avnimelech, 1964). The present view is that the thermal metamorphism is a consequence of the spontaneous subsurface combustion (autometamorphism) of the organic material during the late Miocene (Bentor and Vroman, 1960; Kolodny *et al.*, 1971; Bentor *et al.*, 1972; Kolodny and Gross, 1974). Experimental and chemical studies have indicated an essentially isochemical metamorphism, characterized by decarbonation (Bentor *et al.*, 1972; Kolodny and Gross, 1974). Kolodny and Gross postulate a sequence of events in which the parent sediments were heated, underwent decarbonation at low (approximately atmospheric) pressure and low CO_2 pressure yielding a high-temperature assemblage with spurrite predominant, equivalent to sanidinite to pyroxene hornfels facies. Subsequent cooling with recarbonation and hydration resulted in the appearance of a lower-temperature assemblage, characterized by the pres-

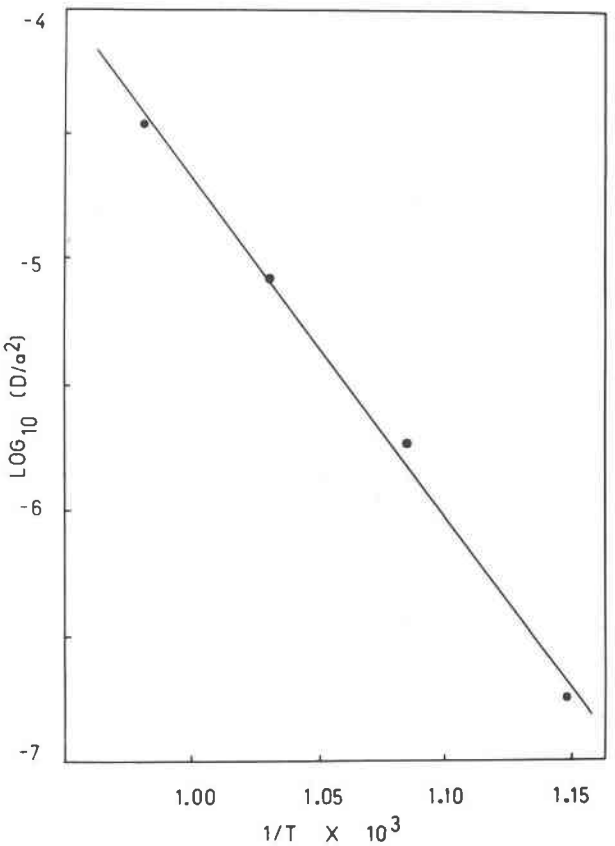

Fig. 6 Arrhenius plot of $\log_{10}(D/a^2)$ against $(1/T) \times 10^3$. Linear regression gives a line of slope -1.36×10^4, intercept 8.93 and correlation coefficient 0.996.

ence of minerals such as ettringite, tobermorite, aragonite, and vaterite.

A particular advantage of the carbonate–fluorapatite decarbonation reaction in geothermometry is that the CO_2 loss is irreversible and not influenced by an retrograde recarbonation. Within the 'Mottled Zone' the mineral is invariably in a state of partial or complete decarbonation, thus emphasizing the high-temperature origin of the assemblage. The highest CO_2 contents (3.2%), found in the margins of the thermal aureole, are significantly lower than the CO_2 contents of the parent sedimentary apatites, which are remarkably constant (3.6–4.0%). The results of $\Delta 2\theta(004)$–(410) measurements correspond very well with the Gross (1976) theory of 'hot spots.' The fluorapatites at such hot spots show almost total CO_2 loss (many show complete loss), whereas they contain progressively more CO_2 as a function of distance from the spots, until the maximum CO_2 contents are obtained in the undisturbed sediments.

The decarbonation data have been extrapolated to lower temperatures by calculating [by means of equation (3) and the experimentally deduced E_A and (D_o/a^2)] values of (D/a^2) at temperatures in the range 300°–600°C. These (D/a^2) values were then inserted into equation (4), and t calculated for known α. The results of this procedure are represented in Figure 7 by a plot of temperature against $\log_{10}t$ (in years) for α values of 0.05, 0.50, and 0.95. The curves give the temperature-time relationships required for the occurrence of the three selected fractional weight losses. The time scale terminates at *ca.* 10,000 years, which is

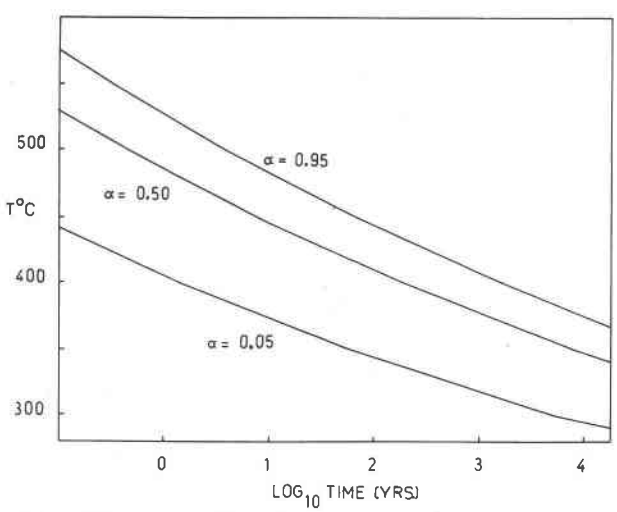

Fig. 7 Temperature–$\log_{10}$ time (in years) plot obtained by the extrapolation of the experimental data to lower temperatures.

an estimate of the maximum life span of the Mottled Zone event calculated from a knowledge of the heat generated by the combustion of the organic matter, the approximate temperatures maintained during the event, and the mass of rock heated. The 0.05 contour represents a minimal CO_2 weight loss (0.2%), and can be used to provide minimum temperature estimates for the metamorphism. It can be seen that even if the 10,000 year life span is chosen, the minimum temperature is shown to be 300°C; if a more conservative estimate of 10–100 years is taken, temperatures in the range 350°–380°C are indicated. Crude decrepitation experiments with Neogene Hazeva sandstones placed the lower temperature limit at 200°–400°C (Kolodny and Gross, 1974). Similarly, the 0.95 contour provides an estimate of the temperatures required for complete decarbonation. However, in this instance the estimates are obviously far too low, since the observed deviations from ideal kinetics at $\alpha \geq 0.75$ render the extrapolations to lower temperatures inaccurate. It should also be noted that any temperature estimates made by this method will tend to be minima, since we do not take into account (1) the grain-size distribution of the naturally occurring apatite, which will be larger than the small size fraction used in this study and (2) CO_2 pressure, which may be more than atmospheric and could inhibit the decarbonation kinetics.

The kinetics of decarbonation also give an indication of optimal conditions for industrial processes which concentrate phosphorites by roasting. Referring to the higher-temperature data in Figure 1, it is evident that a very small fraction of the total heating time results in substantial CO_2 loss. For instance, at 647°C approximately 75 percent of the total CO_2 content is expelled in 20 percent of the time required for 90 percent loss. Since fuel conservation is now an important economic requirement, it may be more economical to partially concentrate the phosphorites by heating at lower temperatures, and for shorter times, than are required for complete decarbonation.

Acknowledgments

We are most grateful to Mrs. Irene Gal for the chemical analyses, to Mrs. Goldstein (Chemical Engineering) of the Hebrew University Microanalysis Laboratory for the Pregl determination, to Mrs. Shulamit Gross for providing the Haturim samples, to Dr. Eytan Sass for the 10,000 year estimate of the Mottled Zone event, and to other colleagues for helpful advice and fruitful discussions. We thank the Negev Phosphate Company for supplying the experimental sample.

References

Altschuler, Z. S., E. A. Cisney and I. S. Barlow (1952). X-ray evidence of the nature of carbonate-apatite (abstr.). *Geol. Soc. Am. Bull., 63,* 1230–1231.

Avnimelech, A. (1964). Remarks on the occurrence of high temperature minerals in the so-called "Mottled Zone" Complex of Israel. *Israel J. Earth Sci., 13,* 102–110.

Bentor, Y. K. and A. Vroman (1960). The Geological Map of Israel, sheet 16: Mount Sdom. *Geol. Surv. Israel,* 117 p.

———, S. Gross and L. Heller (1963a). High temperature minerals in non-metamorphosed sediments in Israel. *Nature, 199,* 478–479.

———, ——— and ——— (1963b). Some unusual minerals from the "Mottled Zone Complex," Israel. *Am. Mineral., 48,* 924–930.

———, ——— and Y. Kolodny (1972). New evidence on the origin of the high-temperature mineral assemblage of the "Mottled Zone" (Israel). *24th Int. Geol. Congr.,* Section 2, 267–275.

Bratton, R. J. and G. W. Brindley (1965). Kinetics of the vapour phase hydration of magnesium oxide. 2. Dependence on temperature and PH_2O. *Trans. Faraday Soc., 61,* 1017–1025.

Carslaw, H. S. and J. C. Jaeger (1959). *Conduction of Heat in Solids.* (2nd Edition). Clarendon Press, Oxford. 510 p.

Carter, R. L. (1961). Kinetic model for solid state reactions. *J. Chem. Phys., 34,* 2010–2015.

Gross, S. (1970). Mineralogy of the 'Mottled Zone' Complex in Israel. List of Minerals. *Israel J. Earth Sci., 19,* 211–216.

——— (1977). Mineralogy of the Haturim Formation, Israel. *Bull. Geol. Surv. Israel, 70,* in press.

———, E. Mazor, E. Sass and I. Zak (1967). The 'Mottled Zone' Complex of Nahal Ayalon (Central Israel). *Israel J. Earth Sci., 16,* 84–96.

Gulbrandsen, R. A. (1970). Relation of carbon dioxide content of apatite of the Phosphoria formation to regional facies. *U.S. Geol. Surv. Prof. Pap. 700 B,* 9–13.

Jander, W. v. (1927). Reaktionen im festen Zustande bei hoheren Temperaturen. *Z. anorg. allgem. Chem., 163,* 1–32.

Kolodny, Y. and S. Gross (1974). Thermal metamorphism by combustion of organic matter. Isotopic and petrological evidence. *J. Geol., 82,* 489–506.

———, M. Bar and E. Sass (1971). Fission track age of the 'Mottled Zone Event' in Israel. *Earth Planet. Sci. Lett., 11,* 269–272.

———, N. Shulman and S. Gross (1973). Hazeva Formation sediments affected by the 'Mottled Zone Event.' *Israel J. Earth Sci., 22,* 185–193.

LeGeros, R. Z., J. P. LeGeros, O. R. Trautz and E. Klein (1970) Spectral properties of carbonate in carbonate-containing apatites. *Dev. Appl. Spectrosc., 7B,* 3–12.

McConnell, D. (1952a). The problem of the carbonate apatites. IV. Structural substitution involving CO_3 and OH. *Bull. Soc. fr. Mineral. Cristallogr., 75,* 428–445.

——— (1952b). The crystal chemistry of carbonate apatites and their relationship to the composition of calcified tissue. *J. Dent. Res., 31,* 53–63.

Martin, B. and W. S. Fyfe (1970). Some experimental and theoretical observations on the kinetics of hydration reactions with particular reference to serpentinization. *Chem. Geol., 6,* 185–202.

Silverman, S. R., R. K. Fuyat and J. D. Weiser (1952). Quantitative determination of calcite associated with carbonate-bearing apatites. *Am. Mineral., 37,* 211–222.

Wynne-Jones, W. F. K. and H. Eyring (1935). The absolute rate of reactions in condensed phases. *J. Chem. Phys., 3,* 492–502.

Manuscript received, March 26, 1976; accepted for publication, October 6, 1976.